

RSC Advances



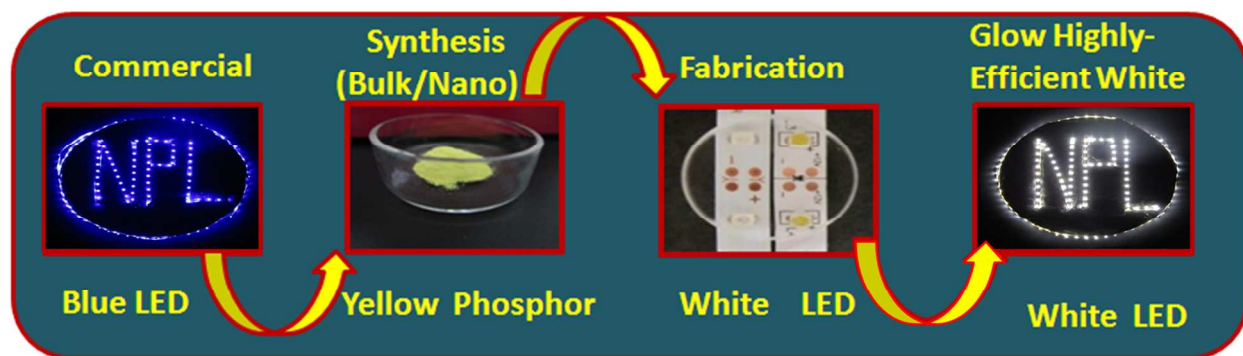
This is an *Accepted Manuscript*, which has been through the Royal Society of Chemistry peer review process and has been accepted for publication.

Accepted Manuscripts are published online shortly after acceptance, before technical editing, formatting and proof reading. Using this free service, authors can make their results available to the community, in citable form, before we publish the edited article. This *Accepted Manuscript* will be replaced by the edited, formatted and paginated article as soon as this is available.

You can find more information about *Accepted Manuscripts* in the [Information for Authors](#).

Please note that technical editing may introduce minor changes to the text and/or graphics, which may alter content. The journal's standard [Terms & Conditions](#) and the [Ethical guidelines](#) still apply. In no event shall the Royal Society of Chemistry be held responsible for any errors or omissions in this *Accepted Manuscript* or any consequences arising from the use of any information it contains.

Graphical Table of Content



A novel approach towards comparative studies of bulk and nano phosphors converted highly-efficient white LEDs.

Commercial approach towards fabrication of bulk and nano phosphors converted highly-efficient white LEDs

Jaya Dwivedi^{†,Π}, Pawan Kumar^{†,Π}, Arun Kumar^{†,Π}, Sudama^{‡,Π}, V.N. Singh^{Φ,Π}, Bhanu Pratap Singh^{‡,Π}, S.K. Dhawan^{Ψ,Π}, V. Shanker^{†,Π} and Bipin Kumar Gupta^{†,Π,*}

[†] Luminescent Materials and Devices Group, Materials Physics and Engineering Division

^Φ Electron and Ion Microscopy Section, Sophisticated Analytical Instruments Division

[‡] Optical Radiation Standards, Apex Level Standards & Industrial Metrology

^Ψ Polymeric and Soft Materials, Materials Physics and Engineering Division

[‡] Physics and Engineering of Carbon, Materials Physics and Engineering Division

^Π CSIR - National Physical Laboratory, Dr. K. S. Krishnan Road, New Delhi, India

Abstract: Herein, we report a strategy to synthesize a highly efficient yellow light emitting $Y_{3-x}Al_5O_{12}: Ce_x$ ($x = 0.03$ to 0.3) based bulk as well as nano (rod shaped) phosphors which is the main component of solid state white light emitting diodes (WLEDs). The as-synthesized phosphors were well characterized by several experimental techniques related to material characterization and spectroscopy. The bulk and nano phosphors are emitting with the maximum photoluminescence intensity peaking at 549 and 530 nm, respectively upon 468 nm excitation wavelength. These phosphors have exhibited higher photoluminescence intensity as compared to commercially available bulk phosphor coated on WLEDs strips. Moreover, the integration of commercially available InGaN blue LED strips with synthesized bulk and nano phosphors demonstrates better CIE coordinates, low colour temperature with high brightness ($>81\%$ quantum yield) as compared to commercially available WLEDs based strips, lantern and torch. These highly efficient light emitting phosphors would be the more feasible and ultimate candidate for their potential use in commercial WLED applications.

Keywords : YAG:Ce, nanorods , white light emitting diodes, photoluminescence, XRD, TEM

* Corresponding author. E-mail address: bipinbhu@yahoo.com , Tel.: +91-11-45609385, Fax: +91-

11- 25726938

1. Introduction

Solid state lighting (SSL) devices have become a paragon source of generating light due to their rapidly improving efficiency with the huge energy saving offered by them as compared to conventional high energy discharge lamp (e.g. metal halides and high pressure sodium) and therefore, requires less input energy to deliver same amount of output power.¹⁻³ Over the past decades, a new generation of solid state lighting in the form of white light-emitting diodes (WLEDs) have fascinated much attention in display and lighting because of their high efficiency, compactness, good material stability, long operational lifetime (>100,000 h) and eco-friendliness which gives them a leading edge over other lighting and display applications.¹⁻⁷ Nowadays, the most general approach to generate white light from LEDs is the combination of blue LEDs (emission at ~460 nm) or near-ultraviolet (N-UV) LEDs (~370–410 nm) with complementary colour emitting phosphors.⁸ Commercially, these are fabricated by combining blue LED chips with yellow-emitting phosphor. The operating mechanism of WLEDs depends upon the optical pumping of the integrated luminophors through emission from coloured LEDs. The subsequent collection of photoluminescence obtained from phosphors preceded by electroluminescence of LEDs determines the properties of device.⁹ To fully exploit WLEDs to their potential, there are still numerous drawbacks which have to be overcome simultaneously to make them feasible in real-life lighting applications. Among them, low colour rendering index ($R_a < 80$) due to deficiency of red colour in emission and different degradation rate of blue LED and phosphor which causes chromatic aberration and poor colour stability are the most critical.¹⁰ Moreover, it emit cool white light having Commission International de l'Eclairage (CIE) coordinates of (0.292, 0.325) and correlated colour temperature (CCT) of 7756 K which aggravates the situation and restricts their use for versatile applications.¹¹

Ever since, WLEDs are based on the combination of yellow phosphor with blue LEDs. Numerous phosphors have been reported including $\text{NaSr}_4(\text{BO}_3)_3:\text{Ce}^{3+}, \text{Mn}^{2+}$, $\text{NaBa}_4(\text{BO}_3)_3:\text{Ce}^{3+}, \text{Mn}^{2+}$, $\text{Sr}_3\text{B}_2\text{O}_6:\text{Ce}^{3+}, \text{Eu}^{2+}$, $\text{LiSrBO}_3:\text{Eu}^{2+}$, $\text{Sr}_3(\text{Al}_2\text{O}_5)\text{Cl}_2:\text{Eu}^{2+}$ and so on for their application for the purpose of WLEDs. Most of them have claimed of their ability to replace $\text{Y}_3\text{Al}_5\text{O}_{12}:\text{Ce}$ (YAG:Ce) in commercial applications but none of them have been successful so far.¹¹⁻¹⁹ Till date, the combination of yellow phosphor YAG:Ce and InGaN based

blue LED is still the most popular method to generate white light.²⁰ The strength of YAG:Ce lies in its unique features such as strong absorption of blue light in range of 440 to 480 nm which results due to dipole-allowed electronic transitions in activated Ce^{3+} ions, subsequent broad emission in yellow region, fast luminescence decay time (< 100 ns), high external quantum efficiency ($\sim 75\%$ under blue LED excitation) and remarkably high chemical and thermal stability.²¹ However, there are still some critical problems associated with commercially used YAG:Ce in WLEDs like harsh synthesis condition, temperature quenching of luminescence and cool light (8500K).²² Recently, many researchers are focusing on development of YAG:Ce nanophosphors to tackle the problems associated with bulk YAG:Ce.²³⁻²⁴ In order to comprehend these proceedings, we have done a comparative study between bulk and nano phosphors in this manuscript. Now, our effort in this present investigation is to address all these issues by tailoring as well as customizing the method for synthesis of both bulk and nano YAG:Ce phosphors. Besides, till date all the recently published literature reports are only focused on the feasibility of either bulk or nano phosphors, not on both simultaneously.²³⁻²⁶ No one has focused their studies on comparison between performance of WLEDs fabricated with bulk and nano phosphors (especially nanorods) of YAG:Ce and their combined comparative study with the commercially available products as per the best of our knowledge which has been accomplished in our present work. Due to their unique structural properties, nanorods are very efficient in extracting light. For efficient operation of WLEDs, larger effective surface area of phosphor with good brightness and minimum lattice distortion are desirable. Nanorods possess both these features. Besides, they have very high aspect ratio which eases the extraction of generated photons. Since, we are utilizing hydrothermal method for preparation of nanorods, the temperature required for their synthesis is also reduced due to higher effective surface area. This leads to a more efficient method of their synthesis causing less power consumption which is further supported by the reduced initial growth temperature for nucleation of the phosphor along with less annealing time. Being light weight in nano form, the gravimetric mass of phosphor required for fabrication of WLEDs is also less in amount. Despite these great advantages, the usages of nanorods based phosphors for practical applications like fabrication of WLEDs are severely restricted because of their lower luminous efficiency and photobleaching as compared to bulk phosphor.²⁷

Concisely, in this paper, we have synthesized bulk as well as nano $\text{Y}_{3-x}\text{Al}_5\text{O}_{12}:\text{Ce}_x$ ($x = 0.03-0.3$) phosphors and integrated them successfully with blue LEDs commercial strip.

Moreover, the shape dependent structural/microstructural studies as well as their photoluminescence properties of synthesized phosphors have been explored in details. Furthermore, comparative studies focused on WLEDs fabricated with bulk and nano YAG:Ce phosphors have been discussed in terms of their commercial use which is merely reported in literature. Besides this, we have also compared in-house fabricated WLEDs strips with commercial available Chinese WLEDs torch (Small Sun) and locally fabricated Lantern (Ashirwad, India) in market. The obtained results significantly assert that our synthesized phosphors can be a promising candidate for replacing existing phosphors utilized in commercial LEDs.

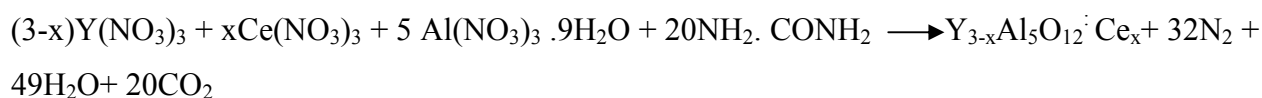
2. Experimental Procedures

We have performed several experiments to synthesize bulk as well as nano YAG phosphor such as solid state reaction, co-precipitation (CP), sol-gel (SG), auto-combustion and hydrothermal methods. But, we got better results in terms of photoluminescent intensity in present investigation (auto-combustion cum solid state diffusion method (for bulk) and hydrothermal reaction (for nano)) as compared to other methods. Thus, we have chosen to explain our best obtained synthesis methods and related results for synthesis of bulk and nano phosphors.

2.1 Preparation of bulk YAG:Ce : Bulk $Y_{3-x}Al_5O_{12}:Ce_x$ ($x = 0.03-0.3$) was prepared by an integrated auto-combustion and solid state diffusion method. The starting materials including Y_2O_3 (99.99%), Al_2O_3 (99.99%) and Ce_2O_3 (99.99%) were used without any further purification unless otherwise stated. All the chemicals were purchased from Sigma Aldrich. Stoichiometric amount of Y_2O_3 , Al_2O_3 and Ce_2O_3 were mixed with minimum quantity of DI water separately so as to form a milky white paste. As it is a well known fact that oxides are insoluble in DI water, therefore, in order to form a transparent solution we have further added few drops of dilute HNO_3 (69% GR) to each of the mixtures separately so as to form nitrates of respective compounds followed by heating at $100^\circ C$ for 2 hrs. under constant stirring. Urea (99.99%) was added to the mixture of prepared metal nitrates solution in 20:1 volume ratio. The concentration of cerium in $Y_{3-x}Al_5O_{12}:Ce_x$ is varied from $x = 0.03$ to 0.3 ; $x = 0.15$ ($Y_{3-x}Al_5O_{12}:Ce_x$) was found

to be optimum value for the synthesis of high quality nano phosphors with high brightness . A typical doping concentration of Ce (x value) is 0.15(5 mol%).

The prepared solution was heated on electric coil heater ($\sim 400^{\circ}\text{C}$). Obtained yellow coloured bulk mass was re-fired in order to get uniform diffusion of Ce in YAG host at 1400°C for 4 hrs in presence of boric acid as flux under ambient conditions. The yield of the product obtained was 88% and it is highly reproducible which can be scaled-up in large quantity. The details about the optimization of Ce concentration and synthesis temperature are well discussed in photoluminescence section. The overall reaction can be summarized as below:



For bulk YAG:Ce , we have used an organic cage of PVA (polyvinyl alcohol) to restrict the agglomeration of particles which is well established in our previous studies for other phosphor material.²⁸ This encapsulation got eliminated at high temperature in the form of CO_2 and H_2O . In case of nanophosphor, we have used cetyl trimethyl ammonium bromide (CTAB) as surfactant which also gets removed from synthesized phosphor when sintered at high temperature. But, we have not incorporated these encapsulants formulae in our main equation in order to maintain discreteness.

2.2 Preparation of nano YAG:Ce : Nanorods of $\text{Y}_{3-x}\text{Al}_5\text{O}_{12}:\text{Ce}_x$ ($x=0.15$) was synthesized by hydrothermal method. The starting materials including Y_2O_3 (99.99%), $\text{Al}(\text{NO}_3)_3 \cdot 9\text{H}_2\text{O}$ (99.99%) and $\text{Ce}(\text{NO}_3)_3$ (99.99%) were used without any further purification unless otherwise stated. All the chemicals were purchased from Sigma Aldrich. Stoichiometric amount of Y_2O_3 , $\text{Al}(\text{NO}_3)_3 \cdot 9\text{H}_2\text{O}$ and $\text{Ce}(\text{NO}_3)_3$ were taken. The metal nitrates were dissolved in DI water to form a transparent solution. As oxides are insoluble in DI water, we have further added dilute HNO_3 (69% GR) into Y_2O_3 paste prepared in DI water to form nitrates of the respective compound. This step was followed by heating at 100°C for 2 hrs. under constant stirring till it became a completely transparent solution. The doping concentration of Ce was kept same as in the case of bulk $\text{Y}_{3-x}\text{Al}_5\text{O}_{12}:\text{Ce}_x$ ($x=0.15$) to compare their responses for the same concentration.. CTAB (1M) was added to the mixture of metal nitrate solutions and then, kept for stirring for 1

hr. which results in a transparent metal nitrate solution. Subsequently, NaOH was added drop wise in the transparent metal nitrate solution without having any sediments and simultaneously stirred vigorously. The pH at the end of this reaction was maintained at ~12. Once yellow precipitate was formed, it floated on the solution and due to continuous stirring, the yellow precipitate got deformed and mixed homogenously with the solution forming a semi dry gel which avoids any kind of sedimentation in the solution. The final solution obtained was kept in a hydrothermal bomb at 185⁰C for 10 hrs. The light weight fine yellowish- white powder obtained after hydrothermal reaction was washed, dried and re-fired at 1400⁰C for 1 hr in presence of boric acid as flux under ambient conditions. The yield of the product obtained in this case was 70% which can be scaled-up in large quantity for commercial purpose.

The synthesis protocols of bulk and nano phosphors are summarized in scheme 1(see supporting information).

2.3 Fabrication of WLEDs strip: A solvent exchange process was developed to disperse the bulk and nanorods phosphors of YAG:Ce in an epoxy resin (structural formula shown in Fig. S1; see supporting information) with appropriate ratio. Epoxy resin has been preferred because of its higher refractive index (1.5) so as to reduce the total internal reflection.²⁹ Initially, we have dispersed YAG:Ce phosphor (in case of bulk YAG:Ce, we have taken approx. 500 mg and in case of nano YAG:Ce, we have taken 10 mg of synthesized powder) in an epoxy solution which is a mixture of epoxy resin and a curing agent (triethylene tetra amine, chemical structural formula shown in Fig. S1; see supporting information) which acts as a hardener. A micro syringe was used for dropping epoxy solution on LED chip The nozzle of syringe which we have used in our experiment was of 0.5mm diameter having drop volume ~ 0.065 mm³. We have kept the amount of epoxy solution used same for both bulk and nano phosphors. The ratio of epoxy resin and hardener was taken to be 100:12.5 by volume. The above mixture was uniformly mixed to make homogeneous mixture. After that, it was carefully dispensed in the empty space available on commercially purchased blue LEDs (LED 60 strip, DC 12 V, SMD Model : 3528; non-waterproof blue InGaN based ROHS, ISO 9001 registered company fabricated, made in China) to fill it properly as shown in scheme 2. Then, it was left without further treatment to get dried at room temperature for few hours before testing. The fabrication protocol of WLEDs from

synthesized bulk and nano phosphors by integrating them with blue LED strips is shown in scheme 2 (see supporting information).

2.4 Characterization of bulk and nano phosphors: As-synthesized bulk and nano phosphors were thoroughly characterized using a number of different techniques. Phase purity identification as well as gross structural characterization of YAG:Ce (bulk and nano) phosphor was performed by XRD technique (Rigaku: MiniFlex, CuK α ; $\lambda=1.5404\text{\AA}$) which utilizes the principle of Bragg Brantano Geometry. The X-ray scan range starts from 20 to 75° at a scanning rate of 2° per minute. Prior to the XRD measurement, calibration of the diffractometer was done with silicon powder ($d_{111}=3.1353\text{\AA}$). Accurate lattice parameters were obtained by a least square fitting method using computer-based unit cell refinement software.³⁰ Scanning electron microscopy (SEM) was performed using Carl Zeiss EVO MA-10 equipment facility. The microstructural characterizations were carried out by TEM and HRTEM (Technai, Model No. G20-twin, 200 kV with super twin lenses having point and line resolutions of 0.144 nm and 0.232 nm, respectively) equipped with energy dispersive X-ray analysis (EDAX) facilities for elemental studies. We checked the chemical composition and presence of element by XPS spectroscopy. The photoluminescence (PL) characterizations of bulk and nano phosphors were carried out using photoluminescence spectrometer (Edinburgh, FLSP- 920) where Xenon flash lamp acts as source of excitation. Time-resolved spectroscopy was performed by photoluminescence spectrometer with EPL 375 nm picoseconds pulsed diode laser as a source of excitation. The PL mapping of bulk and nano phosphors coated blue LEDs strip were performed by WITech alpha 300R+ Confocal PL microscope system (WITech GmBH, Ulm, Germany), where 375 nm diode laser as a source of excitation. To estimate the absolute luminescence quantum efficiency of our synthesized phosphors, we have used an integrating sphere equipped with an Edinburgh spectrometer (model F900) instrument and by measuring the integrated fraction of luminous flux and radiant flux with the standard method, quantum efficiency has been evaluated. The colour temperature, CIE colour coordinates and luminance of the bulk and nano phosphors based WLEDs strips were compared with the commercially available WLEDs by the Colourimeter, C1210, serial no. 1296104, as shown in Fig. S2 and Luminance meter series L1000 as Fig. S3(see supporting information). These instruments facilities are basically part of optical standard unit where national standardization measurement is being done at National Physical Laboratory, New Delhi.

3. Results and Discussions

In the typical synthesis procedure of $Y_{3-x}Al_5O_{12}:Ce_x$ ($x = 0.03-0.3$) phosphors, a customized SSR and Hydrothermal method were used for bulk and nano phosphors, respectively. The main purpose of the modification was to minimize the agglomeration of the bulk and nano particles. We achieved the non-agglomerated phosphors which is the essential requirement for such display applications. The versatility of this method is such that one can easily synthesize large quantity of homogeneous rare-earth doped bulk and nano phosphors for commercial applications.

3.1 Gross structural characterization: The gross structural analyses of the samples were done by powder X-ray diffraction (XRD). Figs. 1(a&b) show the XRD pattern of bulk as well as nanorods of $Y_{2.85}Al_5O_{12}Ce_{0.15}^{3+}$ (YAG:Ce) powder. The XRD analysis is performed to examine the phase purity of bulk and nano phosphors. The obtained experimental XRD patterns of bulk and nano phosphors were well indexed with the Joint Committee on Powder Diffraction Standards (JCPDS) Card No. 33-0040. No additional impurities as well as secondary phases were observed in the XRD patterns. The crystal structural of YAG:Ce exhibited cubic phase with lattice parameter $a=b=c=(12.0218\pm 0.0017)\text{\AA}$ (in case of bulk) and $a=b=c=(11.9634\pm 0.0076)\text{\AA}$ (in case of nano) which belongs to $Ia\bar{3}d$ space group. The lattice parameters for YAG:Ce were calculated from observed 'd' values through a least square fitting method using unitcell refinement software.³⁰ The diffraction peaks were clearly broadened in case of nano YAG:Ce as shown in Fig.1 (b) which was expected according to Scherrer equation

$$\beta = \frac{K\lambda}{\tau \cos \theta} \quad (1)$$

Where β is the line broadening at full width half maximum intensity (FWHM), after subtracting the instrumental line broadening, in radians, τ is the mean size of the crystallites, K is a dimensionless shape factor, which has value close to unity (~ 0.9), λ is the X-ray wavelength, θ is the Bragg angle. The left inset of Fig. 1(a) exhibits the proposed unit cell of $Y_{2.85}Al_5O_{12}Ce_{0.15}^{3+}$ crystal. The right inset shows colour of as-synthesized bulk phosphor under room light. The inset of Fig. 1(b) shows the colour of as-synthesized nano phosphor under room light. The XRD and cell parameters of other variants of $Y_{3-x}Al_5O_{12}:Ce_x$, $x = 0.03$ to 0.3 bulk phosphors are shown in

Fig. S4 and table TS1 (see Supporting Information). It can be noticed that the cell parameters and cell volume are increasing as the concentration of Ce increases up to $x=0.15$ and decreases thereafter. Such characteristic has been previously observed for other rare-earth oxides system in our earlier publication.³⁰ We have also performed Raman as well as FTIR for bulk and nano phosphors as shown in Figs. S5-S8 (see supporting information). The results clearly demonstrates the evidence of YAG:Ce bulk and nano phosphors.³¹⁻³² We have also done the elemental analysis of as-synthesized bulk phosphor by XPS spectroscopy which clearly demonstrated the presence of Al, Y, O and Ce and their valance states as shown in Fig. S9 (see supporting information).

3.2 Surface morphology and microstructural characterizations: Prior to SEM and TEM/HRTEM analysis, we have sonicated the bulk and nano powder samples in ethanol using ultra-sonicator operating at 25 kHz frequency to avoid any kind of the agglomerations in the sample consequently leading to better SEM and TEM/HRTEM image quality.

In order to explore the surface morphology of bulk and nano phosphors of $Y_{2.85}Al_5O_{12}Ce_{0.15}^{3+}$, we performed scanning electron microscopy (SEM). Figs. 2(a &b) represents the SEM images of bulk and nano YAG:Ce phosphors. Figs. 2(c &d) exhibit the magnified version of the marked area in Figs. 2(a &b) by cross red circle. Fig. 2(a) shows the randomly distributed particles having average size $\sim 0.5\mu\text{m}$ (shown by arrow) while nano YAG:Ce has rod shaped structure with dimensions $\sim 1\mu\text{m}$ in length and 20 nm in diameter (shown by arrow). It is well-known from the concepts of carbon nanotubes from which nano rods or nanotubes have evolved that a material having at least one dimension in nano regime which exists till 100 nm will be recognized as nano materials only.³³ The origin of nanorods is due to higher pH maintained (pH \sim 12) during hydrothermal reaction process which leads to conversion of yttrium hydroxide to yttrium hexa-hydroxide having columnar structure. Once, the hexa-hydroxide nanorods formed, this acts as a seed for the growth of oxide nanorods. To analyze the microstructural analysis of synthesized phosphors and to examine their crystal quality, we performed their transmission electron microscopy (TEM) as well as high resolution TEM (HRTEM). Figs. 3 (a &b) shows TEM images of bulk and nano YAG:Ce. In case of bulk YAG:Ce, we get agglomerates of particles having average size $\sim 0.5\mu\text{m}$. In case of nano YAG:Ce, we get nanorods having average diameter of $\sim 20\text{ nm}$ which have good consistency with our SEM data. Typical HRTEM images of the specified area marked by red cross circle in

Figs. 3 (a &b) of bulk and nanorod phosphors respectively of isolated YAG:Ce³⁺ are shown in Figs. 3 (c &d). The precise observation of HRTEM images indicates that the both bulk and nano samples exhibits lattice fringes with an estimated interspacing of 2.68 Å which corresponds to (420) plane. It can be easily noticed from Figs. 3(c &d) that both the samples (bulk and nano phosphors) exhibit the distinct and continuous lattice fringes without having any distortion which confirms the high crystal quality of synthesized phosphors.

3.3 Photoluminescence and time-resolved spectroscopy of YAG:Ce phosphors :

PL characterization of YAG:Ce bulk and nano phosphors were done using a luminescence spectrometer with Xenon lamp as the source of excitation. The concentration of cerium in Y_{3-x}Al₅O₁₂:Ce_x is varied from x = 0.03 to 0.3; x = 0.15 (Y_{2.85}Al₅O₁₂Ce_{0.15}) was found to be optimum value for the synthesis of high quality phosphors with high brightness (see details in supporting information Fig. S10). Fig. S10 shows, initially, a steady increase in the PL intensity with an increase in the Ce concentration up to x = 0.15, however, beyond this optimum value, the PL intensity started to decrease rapidly. This may be due to luminescence quenching owing to excess Ce³⁺ ions. It is well known that the Ce doping concentration can affect the distances between two Ce ions in the host lattice. When the Ce concentration is ≤ 5 mol %, the distance between two Ce ions is far apart and every one of the Ce ions can be regarded as an isolated luminescent center, which independently emits light without any interference. On the other hand, nearby Ce ions can mutually interact by an electric multipolar process due to the shortened distances between two Ce ions in high doping concentration beyond 5 mol %. In the latter case, the energy transfer rates of Ce ions easily exceed the radiative rates. Thus, the absorbed photon energy rapidly migrates among Ce ions in the host lattice, which can decrease the probabilities of the radiative transitions of Ce ions, and even quench the fluorescence if the excited state gets trapped in an energy sink with a high non-radiative deactivation rate constant. This is also known as concentration quenching of fluorescence³⁰. Therefore, it is very crucial to choose an appropriate doping concentration in order to obtain highly efficient photoluminescence when designing lanthanide doped phosphor³⁴.

Once, optimization of concentration was achieved, we carried out experiments further for optimization of growth temperature for perfect phase formation. Growth time and growth temperature are other important parameters that improves the overall crystallinity of the bulk

phosphor without much increase in the size of nanophosphor. To further improve the PL intensity, Fig. S11 shows the dependence of the relative PL peak intensity (emission at 549 nm) on varying growth temperatures as well as growth time. The relative peak intensity and the brightness are increasing when the growth temperature is increased from 900 to 1400°C. However, the PL intensity of the phosphors synthesized at temperatures above 1400 °C decrease sharply as compared to bulk phosphor synthesized at 1400°C (optimum sample). This could be due to the creation of other oxide secondary phases of yttrium and cerium at high temperatures or improper diffusion and placement of Ce³⁺ ions at the unfavorable sites of yttrium.³⁰ The XRD pattern of optimum sample (5 mol %) at high temperature (1500 degree centigrade) where secondary phases of YAP (YAlO₃ having a perovskite structure) and YAM (Y₄Al₂O₉ having a monoclinic structure) have been clearly observed as shown in Fig. S12. The other cause may be that the number of radiative recombinations gradually decreases as compared to non-radiative recombinations after optimum temperature, and the defects in materials form quenching centers, which leads to non-radiative recombination resulting in luminescence quenching³⁰. Therefore, the change in emission intensity should be mainly associated with the defects that come from the surface states of phosphors after the recombination of electron–hole pairs. The crystallization of the phosphor improved with the increase in growth temperature up to optimum temperature (1400°C) and consequently defects decreased accordingly. Further increase in growth temperature leads to increased defects.

Fig. 4(a) show the normalized excitation and emission spectra of bulk Y_{2.85}Al₅O₁₂:Ce_{0.15}³⁺ phosphor having emission wavelength at 549nm corresponding to 468 nm excitation wavelength. The inset of Fig. 4(a) shows the body-colour of as- synthesized bulk phosphor under ordinary light. Fig. 4(b) shows the normalized excitation and emission spectra of nano Y_{2.85}Al₅O₁₂:Ce_{0.15}³⁺ phosphor having emission wavelength at 530nm corresponding to 468 nm excitation wavelength. The inset of Fig. 4(b) shows the body-colour of as- synthesized nano phosphor under ordinary light. Here, the emission of nanophosphors has exhibited a blue-shift than that of bulk phosphor. This blue shift in the PL spectrum of nanophosphors can be understood by the following explanation. Many literatures have reported that the emission and absorption peaks of YAG:Ce phosphor vary with the synthesis method, size of the phosphor particles, doping concentrations and other factors.³⁵ This occurs due to extremely high sensitivity of Ce ion transitions (4f -5d) to the host environment.³⁵ Besides this, it is also a well established

fact that materials while entering into the nano regime exhibit the size dependent blue shift in emission spectra for example ZnO quantum dots or Ag nanoparticles show a blue shift in their emission depending upon their particle sizes. This phenomenon appears due to change in the band-gap of the materials occurring due to quantization of energy levels in case of nano materials as compared to energy bands present in the bulk materials. Here, in the present case, Ce ion doped nanostructures also exhibits the same trend as explained above. In spite of the shifting, both the emission spectra are well located within the yellow region (520nm–580nm) which was desirable as it is complementary to the blue light emitted by blue LEDs to generate white light. Fig. 4(c) shows the chromaticity diagram of CIE colour coordinates for bulk phosphor which is equal to $x=0.4753$ and $y=0.4451$. Fig. 4(d) shows the CIE colour coordinates for nano phosphor which is equal to $x=0.4613$ and $y=0.4321$.

The obtained excitation spectra of bulk YAG phosphor exhibit two peaks at 468nm and 341 nm wavelengths. The existence of these two excitation peaks can be candidly explained by means of energy level diagram of YAG phosphor having Ce^{3+} as its activator as shown in Fig. 5. As we know that Ce is having electronic configuration of $[Xe] 4f^2 6s^2$. Trivalent Ce^{3+} is described by a single electron system having an electronic configuration of $[Xe] 4f^1$. Due to hyperfine splitting which occurs as a consequence of electronic spin and nuclear spin coupling, the ground state of Ce^{3+} ($4f$) splits into two energy levels corresponding to $2F_{7/2}$ state and $2F_{5/2}$ state having an energy difference of about 2200 cm^{-1} (0.28 e V).³⁶ The next higher state corresponds to $5d$ state which splits into many levels under the influence of crystal field. The observed excitation spectra is a consequence of $4f$ - $5d$ dipole allowed transitions. These transitions are extremely sensitive to local environment of Ce^{3+} ion which is basically a substitutional defect³⁶. As a result, there are more than one Ce^{3+} absorption bands in the excitation spectrum but prominently there are two bands corresponding to wavelengths 341 nm and 468nm. The excitation peak occurring between 400 to 500 nm is the most intense and desirable. Because, this is the most essential requirement of a yellow phosphor in order to absorb the emission from InGaN based blue LEDs which lies in the region of 400 to 480 nm. The excitation spectra of YAG:Ce significantly overlaps with the emission spectra of blue LEDs which makes them so functional in fabrication of WLEDs.

Figs. 6 (a & c) show the time-resolved photoluminescence of bulk and nano YAG:Ce phosphors. Time-resolved PL (TRPL) is a non-destructive and powerful technique generally used to determine the excitation lifetime of phosphors which resembles the quality of phosphors. Excitation lifetime is a size dependent parameter. Smaller the size of the phosphor, the shorter would be the excitation lifetime and higher would be its recombination rate.³⁷ For both bulk and nano YAG:Ce, the decay time is in the range of nanoseconds. However, bulk YAG:Ce has larger decay time as compared to nano YAG:Ce. The difference in the decay time of bulk and nano phosphor can be explained by localization of Ce³⁺ ions near surface. Since in nanorods, the surface to volume ratio increases drastically by nanosizing, so large number of Ce³⁺ ions remain localized near surface of nanorods as compared to bulk phosphor. These Ce³⁺ ions act as highly reactive sites due to their higher surface energy. So, there will be very high probability of Ce³⁺ ions oxidizing into Ce⁴⁺ state, thus reducing the absorption as well as optical efficiency of nano phosphors. Besides this, there are large numbers of trap/defect sites available on surface of nanorods which enhances the non-radiative recombinations. As the luminescence decay time (τ) depends on both radiative as well as non-radiative recombinations according to formula ($1/\tau = 1/\tau_{\text{radiative}} + 1/\tau_{\text{non-radiative}}$) which implies that higher the non-radiative recombination rate, faster will be the decay time. Figs. 6 (a & c) exhibits the time-resolved photoluminescence spectrum of bulk and nano Y_{2.85}Al₅O₁₂Ce³⁺_{0.15} phosphors respectively. Figs. 6 (b & d) shows the fitting curve and corresponding parameters for bulk and nano phosphor respectively. The PL decay was recorded for the Ce³⁺ transitions for 549 nm and 530 nm emission corresponding to 375 nm excitation wavelength for bulk and nanophosphor respectively. The lifetime data of Ce³⁺ transitions (549 nm for bulk & 530 nm for nanorod) in Y_{2.85}Al₅O₁₂:Ce_{0.15}³⁺ were very well fitted to a double-exponential function as described by the equation below:

$$I(t) = A_1 \exp(-t/\tau_1) + A_2 \exp(-t/\tau_2) \quad (1)$$

where τ_1 and τ_2 are the decay lifetimes of the luminescence, and A_1 and A_2 are the weighting parameters. The parameters generated from the fitting are listed in figs. 6(b&d). The observed lifetimes for bulk phosphor are $\tau_1 \sim 8.26$ ns and $\tau_2 \sim 53.26$ ns. In case of nanophosphors, the observed lifetimes $\tau_1 \sim 4.56$ ns and $\tau_2 \sim 12.39$ ns. The obtained lifetime results have shown second order exponential decay which have good consistency with earlier published paper on YAG:Ce phosphor.³⁸ However, the value of the decay components depends upon the quality,

composition, intrinsic and extrinsic parameters of the material. For double-exponential decay, the average lifetime, τ_{av} , is determined by the following equation.^[39-42]

$$\tau_{av} = (A_1\tau_1^2 + A_2\tau_2^2) / (A_1\tau_1 + A_2\tau_2) \quad (2)$$

The average lifetime for bulk and nanophosphor are calculated to be $\tau_{av} \sim 48.897$ ns and $\tau_{av} \sim 11.493$ ns, respectively.

Fig. 7(a) exhibits comparative study of normalized PLE spectra of YAG:Ce bulk and nano phosphors excited at 468nm wavelength. It is interesting to observe that bulk phosphor has higher PL intensity as compared to nanophosphor at 1400 degree centigrade growth temperature and 5 mol% concentration of cerium. The obtained results reveal that the bulk phosphor is more suitable for LED application as compared to nano. But, nano has its own advantages due to less gravimetric mass which compensate its lower intensity by using less incorporation (50 times less than bulk sample) of nanomaterial for fabrication of LEDs. We also performed the photo-beaching experiment of bulk and nano phosphors. The obtained results reveal that both phosphor exhibits better stability of photoluminescence as shown in Figs. S(13&14). Keeping commercial approach in view, the comparative study has been performed among the synthesized bulk and nano phosphors with commercial YAG:Ce bulk phosphor (synthesized using solid state reaction) obtained from uncoated white LED strips. Fig. 7(b) exhibits the comparison of normalized PL (fixed at 468nm excitation wavelength) and PLE spectra (fixed at 549 nm emission wavelength) of bulk, nano and commercial YAG:Ce bulk phosphor coated on WLED commercial strip(LED 60 strip, DC 12 V, SMD Model : 3528; non-waterproof blue InGaN based ROHS, ISO 9001registered company fabricated, made in China). In order to maintain the consistency, we have compared the as-synthesized phosphor and in-house fabricated WLEDs with same company based commercial YAG:Ce bulk phosphor which is coated on commercial WLED strip and commercial WLED strip respectively. The PL emission intensity outcome of the comparative study portrays the feasibility of synthesized phosphors (bulk and nano) for their commercial use in white LEDs applications. Fig. 7(c) shows the comparison of CIE coordinates of bulk and nano phosphor. Fig. 7(d) shows the comparison of CIE coordinates of bulk, nano and commercially available YAG phosphor.

3.4 Electroluminescence studies of phosphor converted WLEDs (pc-WLEDs) Strips (in-house fabricated and commercially available):

In order to explore the electroluminescence (EL) studies of pc-WLEDs, in-house fabricated bulk and nano phosphors converted white LEDs strips were compared with the commercial available white LEDs strips at 12 volt DC power supply. For the precise measurement of EL, we placed fabricated strips on PL holder keeping the other region covered by black paper except single LED as shown in Fig. S15. The position of exposure of LED is also optimized by employing the visible green emission 532 nm during experiment as shown in Fig. S15. As we know that the LEDs emission intensity is quite high, we placed quartz diffuser in front of strips throughout experiment to prevent the saturation of PMT detector.

Figs. 8 (a &b) represent the EL emission spectra of commercial blue LEDs strips without phosphor coating at 12 volt DC (glowing mode). The EL emission spectra of Figs. 8 (a &b) exhibit the emission wavelength at 460 nm upon 12 volt DC supply. The EL emission spectra of blue LED significantly overlaps with excitation spectra of bulk and nano phosphor powder based spectra as shown in Figs. 4(a &b) which implies that this excitation wavelength is perfectly suitable for making device for white light generation through blue strips. The inset of Figs. 8(a &b) represent the uncoated blue strips as well as bulk and nanophosphor coated blue LED strips respectively. Figs. 8 (c &d) display the EL emission spectra of in-house fabricated bulk and nano phosphors coated blue LED at 12 volt DC power supply respectively. The EL emission spectra reveal the white light conversion from blue LEDs through yellow phosphors. The right inset of Figs. 8(c &d) show the bulk and nano phosphor coated blue strips emitting highly efficient white light. In order to examine the uniformity of phosphor coating on blue LED strips, we have performed PL mapping. The obtained results confirm the highly efficient photoluminescence intensity with uniform distribution throughout the surface as shown in left inset of Figs. 8(c &d) along with the scale bar.

Finally, we demonstrate the comparative study on white light emission from bulk and nano phosphors of YAG: Ce coated blue LED strips with commercial white LED strip as shown in Fig. 9(a). It is evident from this EL emission spectra that indigenously made phosphor shows encouraging results due to its high PL intensity as well as better CIE coordinates as compared to commercial one which creates new hope for commercial applications. Fig. 9(b) represents a comparison of CIE coordinates of bulk, nano phosphor coated WLEDs with commercial WLEDs

strip. Figs. 9(c)-(i-ii) demonstrates the commercial available pristine blue LED without and with 12V DC power supply with alphabet NPL. (iii-iv) portraits the bulk yellow phosphor coated blue LED without and with 12V DC power supply. The photographs elucidate the highly efficient WLEDs strips after phosphor integration. Furthermore, we also compared the performance of bulk and nano phosphors of YAG: Ce coated blue LED strips with commercially available WLEDs strip, Lantern and Torch, for proposed commercialization of our products as shown in table 1. In-house fabricated devices show the lower colour temperature with better CIE coordinates and CRI as compared to commercial product available in market which represents these phosphors have ultimate potential to replace commercially available phosphor.

4. Conclusions

In summary, we have successfully synthesized the bulk phosphor by integrated auto-combustion cum solid state diffusion method. Nano phosphor (rod shaped) has been synthesized via hydrothermal route. The choice of the host material (i.e. YAG) as well as activator (Ce) is adequately justified. The reaction conditions were simple and effective with more than 88% yield of synthesis in case of bulk phosphor and 70% in case of nano phosphors, which can be easily scaled-up in large quantities. These phosphors have exhibited higher photoluminescence intensity with more than 81% estimated quantum yield for bulk and 72% for nano phosphors which are higher than commercially available bulk phosphor. Furthermore, the commercially available InGaN blue LED strips integrated with synthesized yellow bulk and nano phosphors demonstrates better CIE coordinates(bulk~0.32,0.34;nano~0.31,0.35), lower colour temperature (CCT) (bulk~6085K,nano~6350K), higher luminous efficiency (η) (bulk~76.13 lmW^{-1} , nano~69.60 lmW^{-1}) and better colour rendering index(Ra) (bulk~88; nano~82) with high brightness as compared to commercially available WLEDs based strips, lantern and torch. The synthesis of bulk and nano phosphor for WLEDs in this work offers a new paradigm shift in the engineering of WLEDs for commercial applications. We envision that such accomplishments will be the key to develop the high performance applications of bulk and nano phosphors based WLEDs instead of commercially available WLEDs phosphors.

Acknowledgments

The authors wish to thank Prof. R. C. Budhani, Director, N.P.L., New Delhi for his keen interest in the work. The authors are thankful to Prof. O.N. Srivastava (Banaras Hindu University, Varanasi) for his encouragement. The authors also thank Dr. V.P.S. Awana and K. N. Sood for recording XRD pattern and SEM micrograph, respectively. Jaya Dwivedi and Pawan Kumar thank to CSIR and UGC for providing financial assistance.

References

1. J. S. Kim, P. E. Jeon, J. C. Choi, H. L. Park, S. I. Mho and G. C. Kim, *Appl. Phys. Lett.*, 2004, **84**, 2931.
2. W. B. Im, Y. I. Kim, N. N. Fellows, H. Masui, G. A. Hirata, S. P. Den and B. R. Seshadri, *Appl. Phys. Lett.*, 2008, **93**, 091905.
3. T. Nishida, T. Ban and N. Kobayashi, *Appl. Phys. Lett.*, 2003, **82**, 3817.
4. S. Nakamura and G. Fasol, *The Blue Laser Diode*, Springer, Berlin, 1997.
5. H. V. Demir, U. O. S. Seker, G. Zengin, E. Mutlugun, E. Sari, C. Tamerler and M. Sarikaya, *ACS nano*, 2011, **5**, 2735.
6. A. A. Setlur, W. J. Heward, Y. Gao, A. M. Srivastava, R. G. Chandran and M. V. Shankar, *Chem. Mater.*, 2006, **18**, 3314.
7. Y. D. Huh, J. H. Shim, Y. Kim and Y. R. Do, *Journal of Electrochem. Soc.*, 2003, **150**, 57.
8. H. S. Jang, Y. H. Won and D. Y. Jeon, *Appl. Phys. B: Laser Opt.*, 2009, **95**, 715.
9. X. M. Zhang, X. B. Qiao and H. J. Seo, *Curr. Appl. Phys.*, 2011, **11**, 442.
10. X. M. Zhang and H. J. Seo, *Physica B*, 2010, **405**, 2436.
11. C. K. Chang and T. M. Chen, *Appl. Phys. Lett.*, 2007, **91**, 081902.
12. Z. J. Wang, P. L. Li, Z. P. Yang, Q. L. Guo, and X. Chin. Li, *Phys. B*, 2010, **19**, 017801.
13. Y. S. Tang, S. F. Hu, W. C. Ke, C. C. Lin, N. C. Bagkar and R. S. Liu, *Appl. Phys. Lett.* 2008, **93**, 131114.
14. J. H. Yum, S. Y. Seo, S. Lee, and Y. E. Sung, *Proc. SPIE*, 2001, **4445**, 60.
15. Y. S. Lin, R. S. Liu, and B. M. Cheng, *J. Electrochem. Soc.*, 2005, **152**, J41.

16. J. H. Yum, S. Y. Seo, S. Lee, and Y. E. Sung, *J. Electrochem. Soc.*, 2003, **150**, H47.
17. S. Lee and S. Y. Seo, *J. Electrochem. Soc.*, 2002, **149**, J85.
18. P. Shlotter, J. Baur, C.H. Hielscher, M. Kunzer, H. Obloh, R. Schmidt and J. Schneider, *Mater. Sci. Eng.*, 1999, **B59**, 390.
19. J. Baur, P. Shlotter, J. Schneider and Festkörperprobleme, *Adv. Solid State Phys.*, 1998, **37**, 67.
20. P. Shlotter, R. Schmidt and J. Schneider, *Appl. Phys. A*, 1997, **64**, 417.
21. J. K. Park, C. H. Kim, S. H. Park and H. D. Park, *Appl. Phys. Lett.*, 2004, **84**, 1647.
22. Volker Bachmann, Cees Ronda and Andries Meijerink, *Chem. Mater.*, 2009, **21**, 2077
23. Tetsuhiko Isobe, *ECS Journal of Solid State Science and Technology*, 2013, **2**, R3012
24. H.J. Yang, H.R. Xu, G.S. Zhu, L. Yuan, C. Zhang, F.S. Li, A.B. Yu, *Materials Letters*, 2013, **92**, 161
25. Sang Ho Lee, Hye Young Koo, Su Min Lee and Yun Chan Kang, *Ceramics International*, 2010, **36**, 611
26. Heesun Yang, Dong-Kyoon Lee and Yong-Seog Kim, *Materials Chemistry and Physics*, 2009, **114**, 665
27. A. Revaux, G. Dantelle, N. George, R. Seshadri, T. Gacoin, J. Boilot, *Nanoscale*, 2011, **3**, 2015
28. B.K. Gupta, T. N. Narayanan, S. A. Vithayathil, Y. Lee, S. Koshy, A. L. Mohana Reddy, A. Saha, V. Shanker, V.N. Singh, B. A. Kaiparettu, A. A. Martí, and P. M. Ajayan; *Small*, 2012, **8**, 3028.
29. Wei-Fang Su, Ya-Ching Fu and Wei-Ping Pan, *Thermochimica Acta*, 2002, **392–393**, 385.
30. B. K. Gupta, D. Haranath, S. Saini, V. N. Singh, V. Shanker, *Nanotechnology*, 2010, **21**, 055607.
31. Peter Lasch, Antje Hermelink and Dieter Naumann, *Analyst*, 2009, **134**, 1162.
32. Ryo Asakura, Tetsuhiko Isobe, Kiyoshi Kurokawa, Hideki Aizawa and Michio Ohkubo *Anal Bioanal Chem*, 2006, **386**:1641.
33. Juh Tzeng Lue, *Encyclopedia of Nanoscience and Nanotechnology*; Edited by H. S. Nalwa, 2007, **X**, 1.

34. B.K. Gupta, V. Rathee, T. N. Narayanan, P.Thanikaivelan, A. Saha, Govind, S.P. Singh, V. Shanker, A. A. Marti, and P. M. Ajayan, *Small*, 2011,**7**, 1767.
35. Dongdong Jia, *Chemical Engineering Communications*, 2007, **194:12** , 1666
36. Y. Pan, M. Wu, Q. Su, *Journal of Physics and Chemistry of Solids*, 2004,**65**,845.
37. B.K. Gupta , V. Shanker, M. Arora, and D. Haranath, *Applied Physics Letters*, 2009,**95** 073115 31.
38. J.D. Furman, G. Gundiah, K. Page, N. Pizarro, A.K. Cheetham, *Chemical Physics Letters*, 2008,**465**, 67.
39. Q. Lu, Y. Wu, L. Ding, G. Zu, A. Li, Y. Zhao, H. Cui, *J. Alloys Compd.*, 2010, **496**, 488.
40. S. Murakami, M. Herren, D. Rau and M. Morita, *Inorg. Chim. Acta*, 2000,**1014**, 300.
41. T. Fujii, K. Kodaira, O. Kawauchi, N. Tanaka, *J. Phys. Chem. B*,1997, **101**, 10631.
42. B.K. Gupta, P.Thanikaivelan, T. N. Narayanan, L. Song, W. Gao, T.Hayashi, A.L.M. Reddy, A. Saha, V.Shanker, M. Endo, A. A. Martí and P. M. Ajayan, *Nano Letters*, 2011,**11**, 5227.

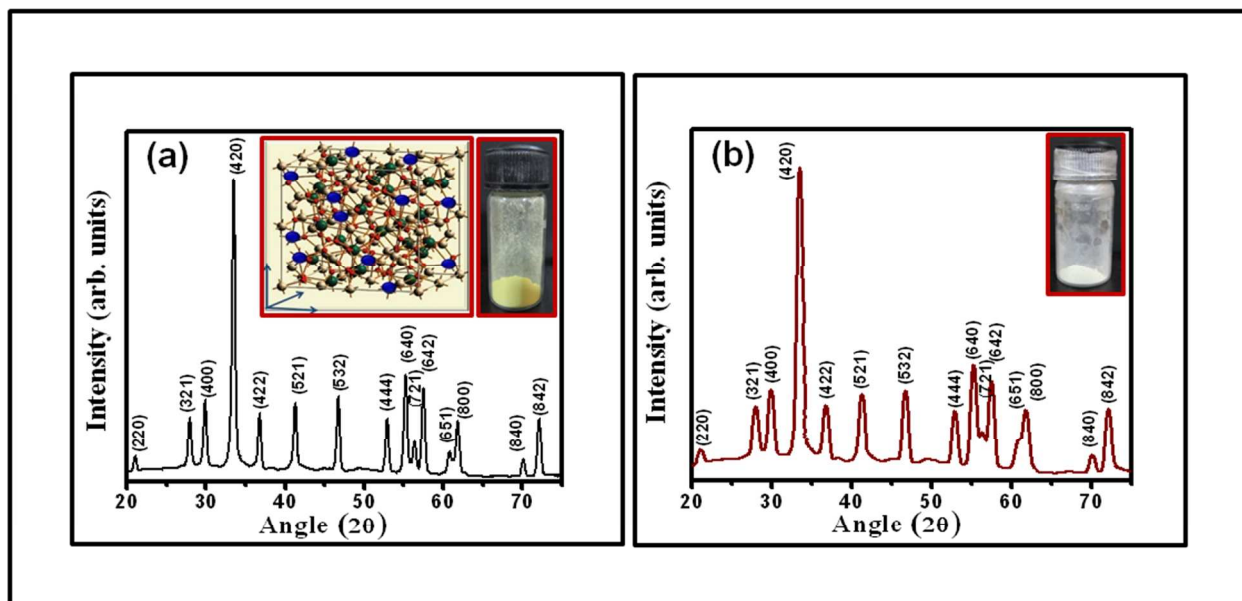


Fig. 1

Fig. 1: a) shows the XRD pattern of bulk $Y_{2.85}Al_5O_{12}Ce^{3+}_{0.15}$ phosphor, XRD pattern is indexed using JCPDS Card No.33-0040. Left inset shows the proposed unit cell of Ce doped YAG crystal. Green, blue, whitish grey and red sites are occupied by yttrium, cerium, aluminium and oxygen, respectively. All together, the unit cell composed of eight molecular units of $Y_{2.85}Al_5O_{12}Ce^{3+}_{0.15}$. Cerium atoms (blue colour) occupy yttrium sites substitutionally. Right inset shows as-synthesized bulk phosphor. **b)** Fig. shows the XRD of nano $Y_{2.85}Al_5O_{12}Ce^{3+}_{0.15}$ phosphor. Inset shows the as-synthesized nano phosphor.

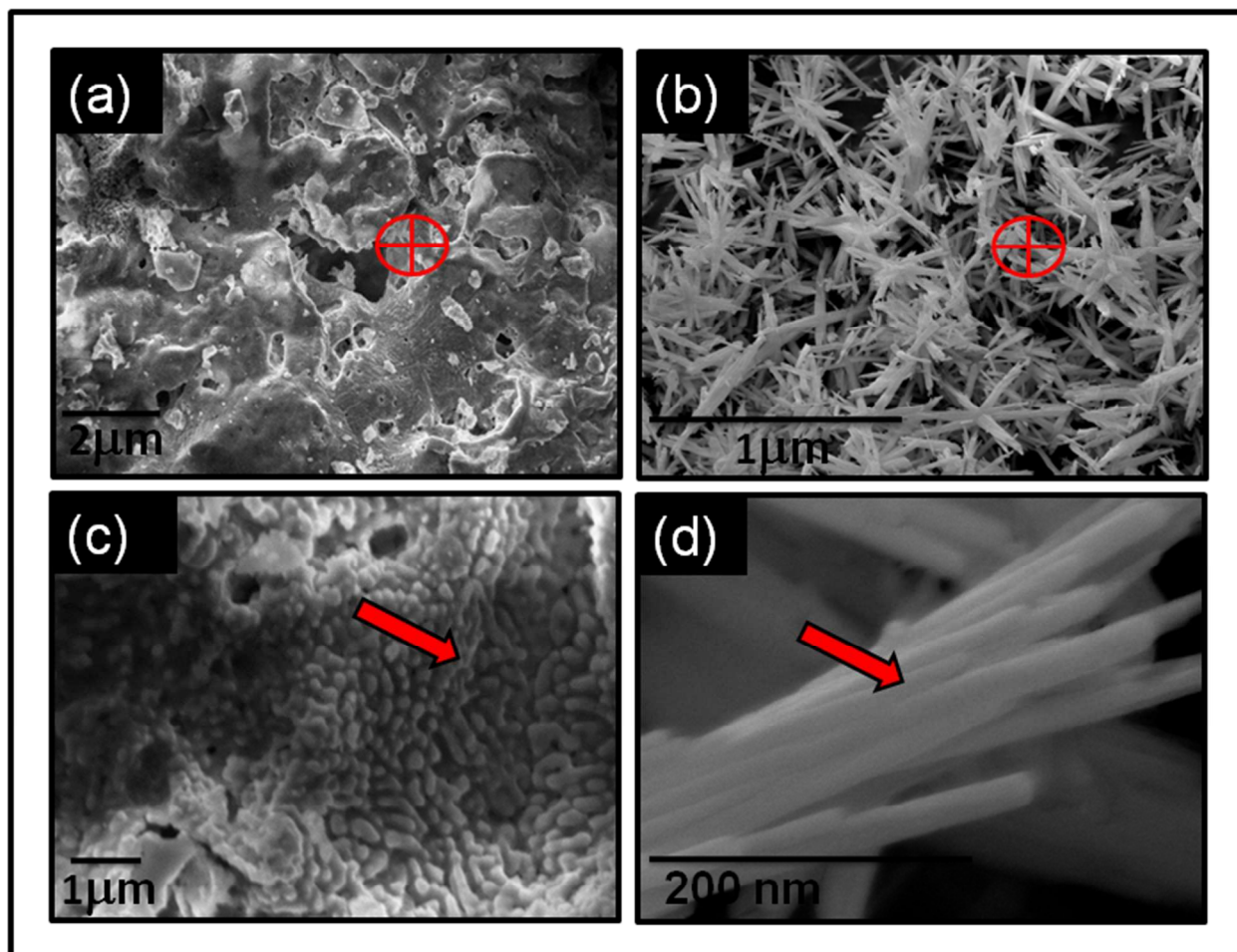


Fig. 2

Fig. 2 : (a) SEM micrograph of bulk $Y_{2.85}Al_5O_{12}Ce^{3+}_{0.15}$ phosphors. (b) SEM micrograph of nano $Y_{2.85}Al_5O_{12}Ce^{3+}_{0.15}$ phosphors. (c) magnified view of $Y_{2.85}Al_5O_{12}Ce^{3+}_{0.15}$ bulk phosphors. (d) magnified view of nano $Y_{2.85}Al_5O_{12}Ce^{3+}_{0.15}$ phosphors.

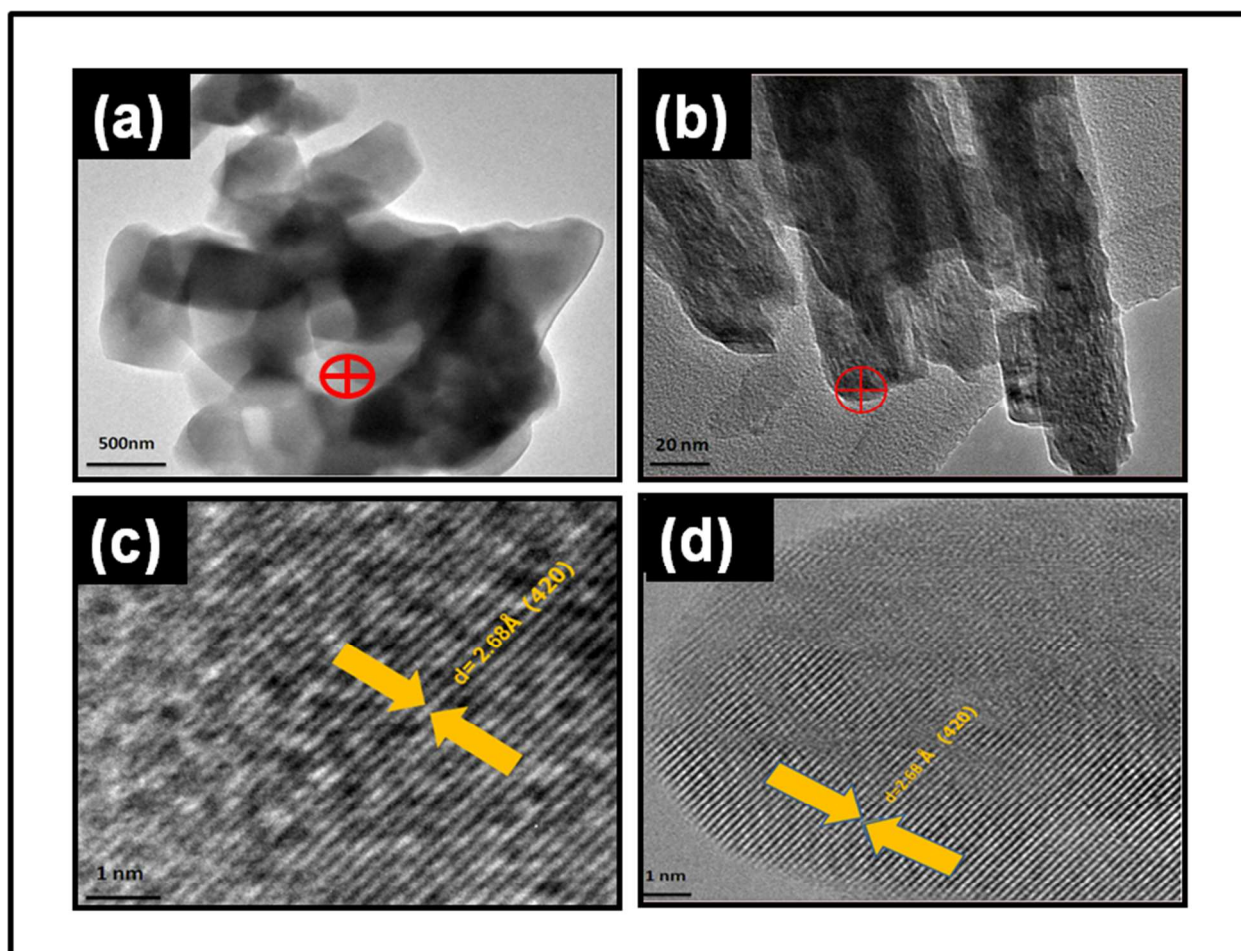


Fig. 3

Fig. 3: (a) TEM micrograph of bulk $\text{Y}_{2.85}\text{Al}_5\text{O}_{12}\text{Ce}^{3+}_{0.15}$ phosphors (b) TEM micrograph of nano $\text{Y}_{2.85}\text{Al}_5\text{O}_{12}\text{Ce}^{3+}_{0.15}$ phosphors (c) HRTEM image of bulk $\text{Y}_{2.85}\text{Al}_5\text{O}_{12}:\text{Ce}^{3+}_{0.15}$ (d) HRTEM image of nano $\text{Y}_{2.85}\text{Al}_5\text{O}_{12}:\text{Ce}^{3+}_{0.15}$.

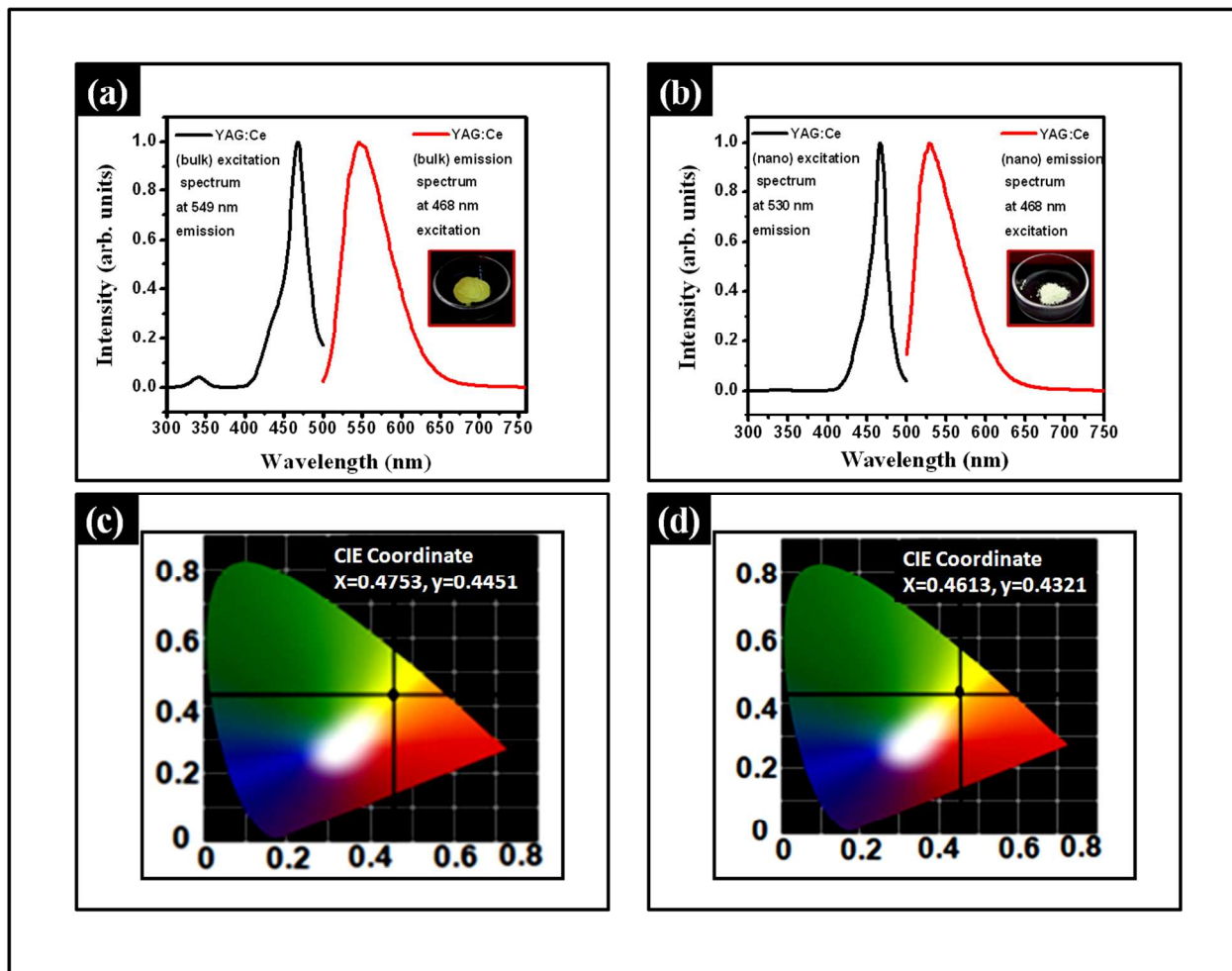


Fig. 4

Fig. 4: (a) Normalized excitation and emission spectra of bulk $Y_{2.85}Al_5O_{12}:Ce_{0.15}^{3+}$ phosphor. The inset exhibits yellow body colour of as-synthesized bulk phosphor under ordinary light. (b) Normalized excitation and emission spectra of nano $Y_{2.85}Al_5O_{12}:Ce_{0.15}^{3+}$ phosphors and its inset shows white colour powder of as-synthesized nano phosphor under ordinary light (c) CIE coordinates of bulk $Y_{2.85}Al_5O_{12}:Ce_{0.15}^{3+}$ phosphors (d) CIE coordinates of nano $Y_{2.85}Al_5O_{12}:Ce_{0.15}^{3+}$ phosphors.

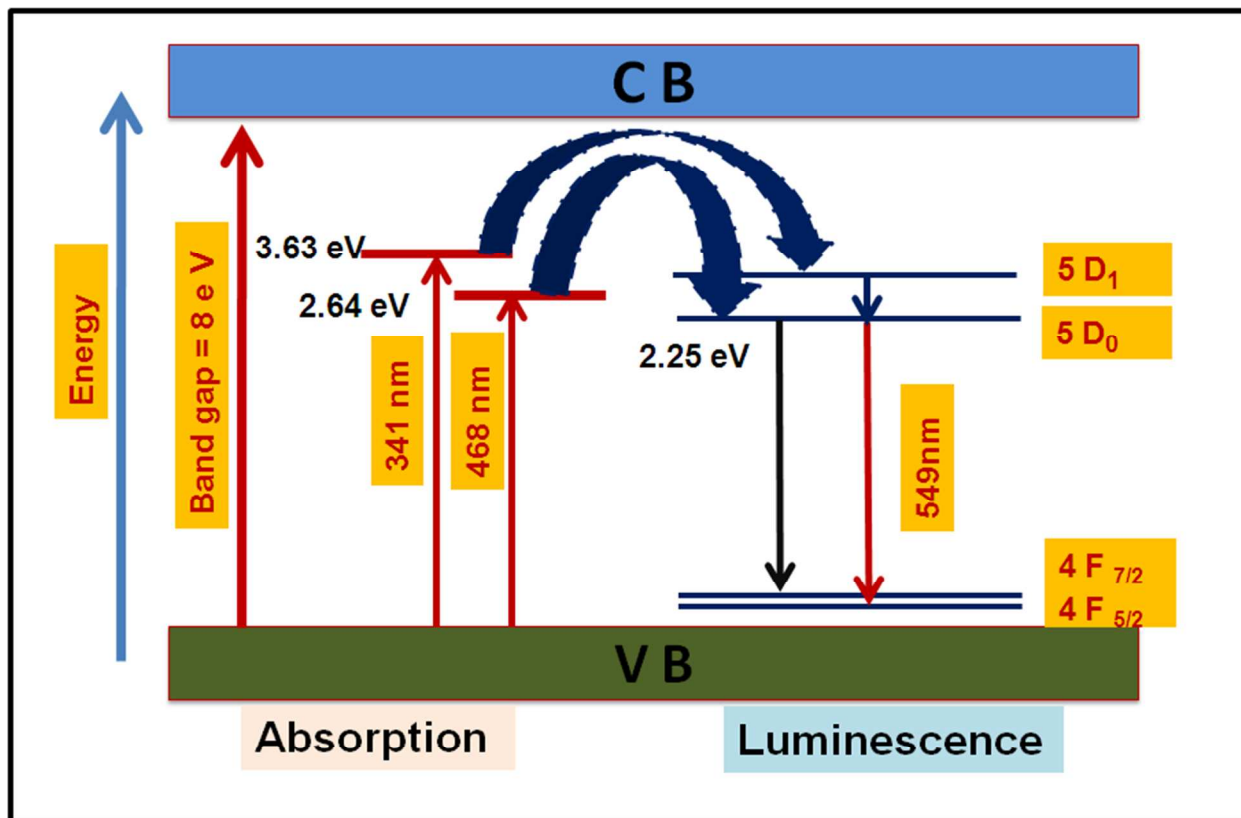


Fig. 5

Fig. 5: Proposed energy level diagram of $\text{Y}_3\text{Al}_5\text{O}_{12}:\text{Ce}^{3+}$.

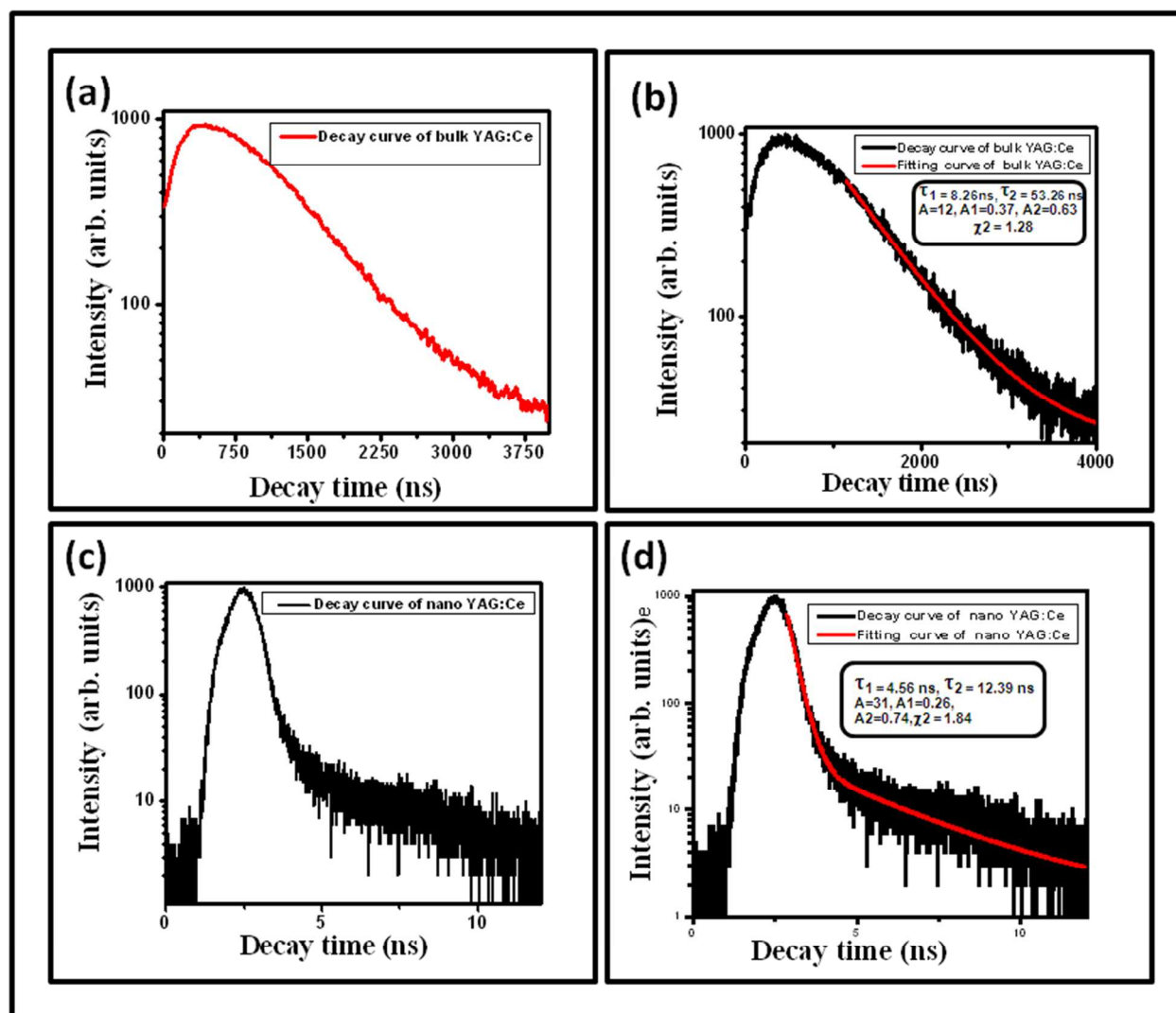


Fig. 6

Fig. 6: (a) Time-resolved photoluminescence spectrum of bulk $\text{Y}_{2.85}\text{Al}_5\text{O}_{12}\text{Ce}^{3+}_{0.15}$ phosphors. (b) shows the fitting curve and corresponding parameters for bulk phosphor. (c) Time-resolved photoluminescence spectrum of nano $\text{Y}_{2.85}\text{Al}_5\text{O}_{12}\text{Ce}^{3+}_{0.15}$ phosphors. (d) shows the fitting curve and generated parameters of nanophosphor.

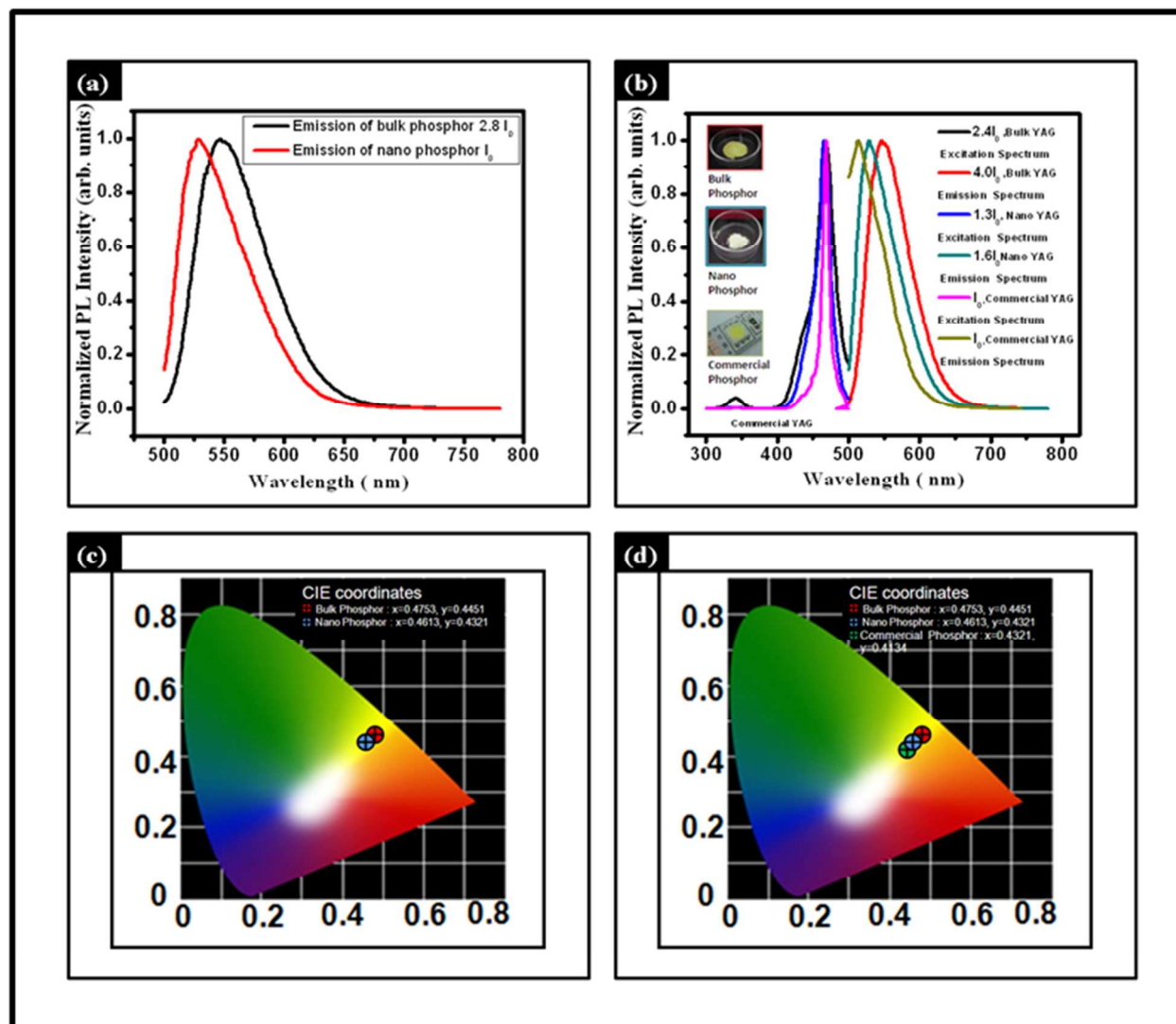


Fig.7

Fig. 7: (a) Comparison of normalized PL emission spectra of YAG:Ce (bulk and nano) phosphors at 468nm excitation wavelength. (b) Comparison of normalized PLE and PL spectra of bulk (as-synthesized), nano (as-synthesized) and commercial available YAG:Ce bulk phosphor. (c) Comparison of CIE coordinates of bulk and nano phosphor (d) Comparison of CIE coordinates of bulk, nano and commercially available phosphor

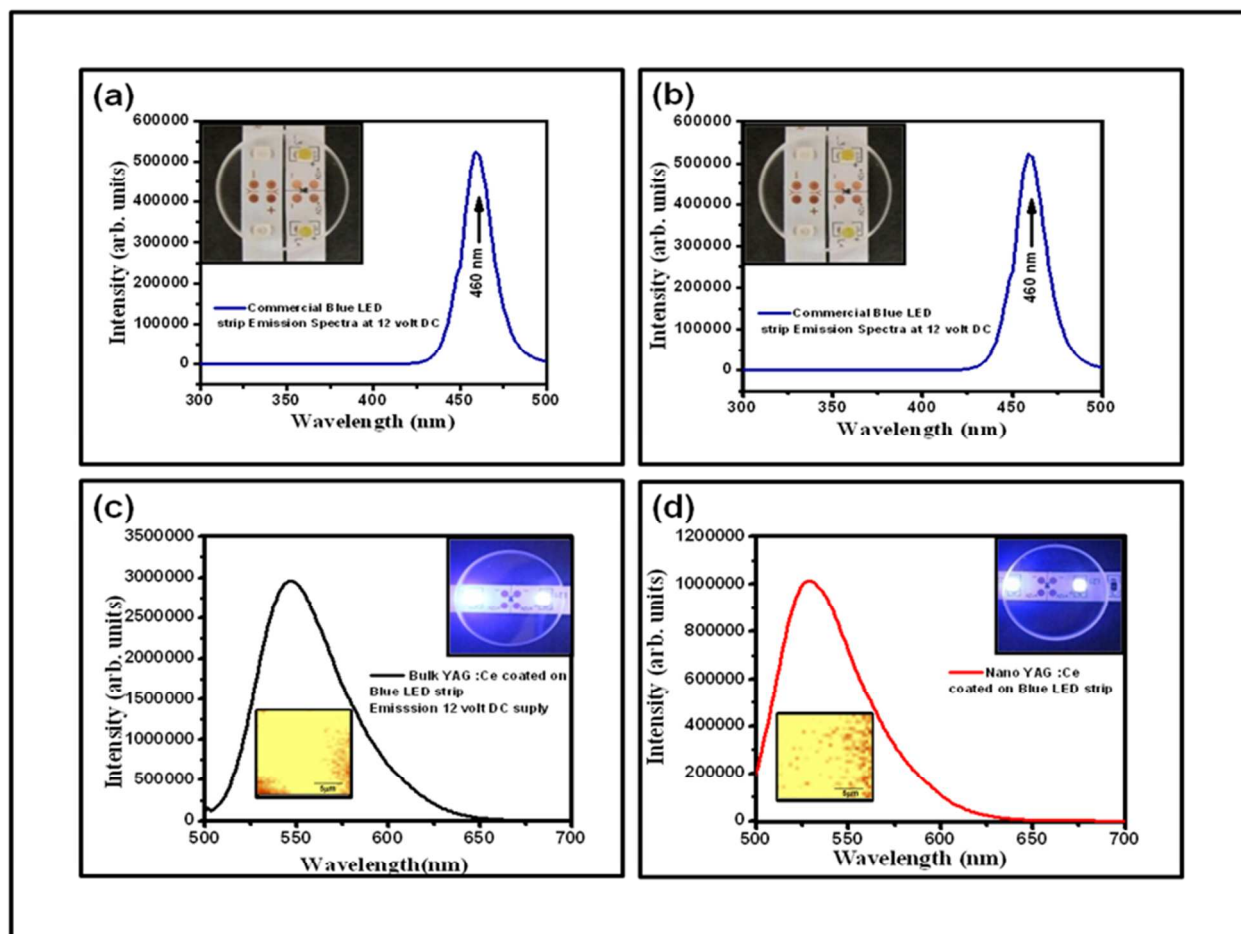


Fig. 8

Fig. 8 : (a&b) represents the EL emission spectra of commercial blue LEDs strips without phosphor coated at 12 volt DC voltage (glowing mode) while inset show the blue LED without and with bulk and nano phosphors coated strips respectively. (c&d) display the white light EL emission spectra of in-house fabricated bulk and nano phosphors coated blue LED at 12 volt DC power supply while the right inset of (c&d) show the bulk and nano phosphor coated blue strips emitting highly efficient white light. Left inset of (c&d) portraits PL mapping image of bulk and nano phosphor coated blue LEDs.

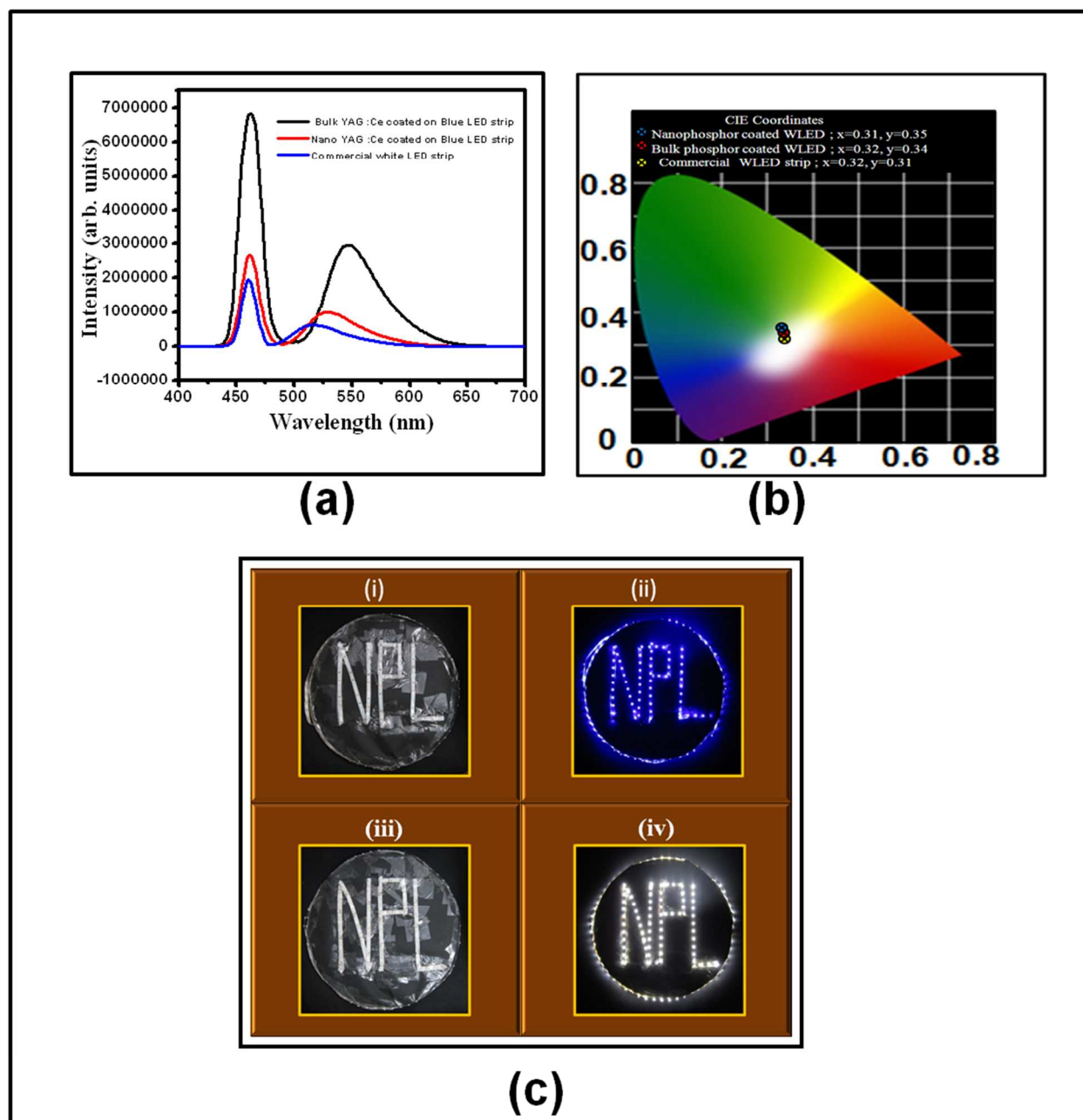


Fig. 9

Fig. 9: (a) Comparative studies between EL spectra of commercial and in-house developed white LEDs to explore feasibility of as-synthesized bulk and nano phosphor. (b) Comparison of CIE coordinates of bulk, nano phosphor coated WLEDs and commercial WLEDs strip (c) (i-ii) demonstrates the commercial available blue LED strip without and with 12V DC power supply. (iii-iv) portraits the bulk yellow phosphor coated on blue LED strip without and with 12V DC power supply.







Sources	Samples	CCT	CIE	Luminance
	Ideal white light	5500 K	(0.33, 0.33)	
	Commercial LED (YAG:Ce)	7181 K	(0.32, 0.31)	2.3 cd/m ²
	Synthesized Bulk YAG:Ce Integrate with blue LED strips	6350 K	(0.32, 0.34)	20 cd/m ²
	Synthesized Nano YAG:Ce Integrate with blue LED strips	6085 K	(0.31, 0.35)	7.4 cd/m ²
	Commercial Lantern	11500 K	(0.28, 0.28)	1.4 x 10 ⁴ cd/m ²
	Commercial Torch	8300 K	(0.29, 0.27)	2.07 x 10 ² cd/m ²

Table 1

Table 1: Performance comparison of as-synthesized bulk and nano phosphors of YAG: Ce coated blue LED strips with commercially available WLEDs strip, Lantern and Torch for proposed commercialization approach of our products.